

Alma Mater Studiorum Università di Bologna
Archivio istituzionale della ricerca

Intertumoral Heterogeneity within Medulloblastoma Subgroups

This is the final peer-reviewed author's accepted manuscript (postprint) of the following publication:

Published Version:

Cavalli F.M.G., Remke M., Rampasek L., Peacock J., Shih D.J.H., Luu B., et al. (2017). Intertumoral Heterogeneity within Medulloblastoma Subgroups. *CANCER CELL*, 31(6), 737-754.e6 [10.1016/j.ccell.2017.05.005].

Availability:

This version is available at: <https://hdl.handle.net/11585/720789> since: 2020-02-03

Published:

DOI: <http://doi.org/10.1016/j.ccell.2017.05.005>

Terms of use:

Some rights reserved. The terms and conditions for the reuse of this version of the manuscript are specified in the publishing policy. For all terms of use and more information see the publisher's website.

This item was downloaded from IRIS Università di Bologna (<https://cris.unibo.it/>).
When citing, please refer to the published version.

(Article begins on next page)



Published in final edited form as:

Circ Res. 2018 May 11; 122(10): e75–e83. doi:10.1161/CIRCRESAHA.117.312082.

Desmin Phosphorylation Triggers Preamyloid Oligomers Formation and Myocyte Dysfunction in Acquired Heart Failure

Peter P. Rainer^{1,2}, Peihong Dong², Matteo Sorge³, Justyna Fert-Bober⁴, Ronald J. Holewinski⁴, Yuchuan Wang², Catherine A. Foss², Steven S. An⁵, Alessandra Baracca⁶, Giancarlo Solaini⁶, Charles G. Glabe⁷, Martin G. Pomper², Jennifer E. Van Eyk⁴, Gordon F. Tomaselli², Nazareno Paolocci^{2,8}, and Giulio Agnetti^{2,6}

¹Medical University of Graz, Graz, Austria

²Johns Hopkins School of Medicine, Baltimore, MD, US

³University of Turin, Turin, Italy

⁴Cedars-Sinai Medical Center, Beverly-Hills, CA, US

⁵Johns Hopkins School of Public Health, Baltimore, MD, US

⁶DIBINEM, University of Bologna, Bologna, Italy

⁷University of California Irvine, CA, USA

⁸University of Perugia, Perugia, Italy

Abstract

Rationale—Disrupted proteostasis is one major pathological trait that heart failure (HF) shares with other organ proteinopathies, such as Alzheimer’s and Parkinson’s diseases. Yet, differently from the latter, whether and how cardiac preamyloid oligomers (PAOs) develop in acquired forms of HF is unclear.

Objective—We previously reported a rise in mono-phosphorylated, aggregate-prone desmin in canine and human HF. We now tested if mono-phosphorylated desmin acts as the seed nucleating PAOs formation and determined if positron emission tomography (PET) is able to detect myocardial PAOs in non-genetic HF.

Methods and Results—Here, we first show that toxic cardiac PAOs accumulate in the myocardium of mice subjected to transverse aortic constriction (TAC), and that PAOs co-migrate with the cytoskeletal protein desmin in this well-established model of acquired HF. We confirm this evidence in cardiac extracts from human ischemic and non-ischemic HF. We also demonstrate that Ser-31 phosphorylated (pSer31) desmin aggregates extensively in cultured cardiomyocytes. Lastly, we were able to detect the in vivo accumulation of cardiac PAOs using positron emission tomography (PET) for the first time in acquired HF.

Address correspondence to: Dr. Giulio Agnetti, Cardiology, Johns Hopkins School of Medicine, 720 Rutland Ave., Ross 1042, Baltimore, MD 21205, USA, Tel: 443-287-7490, Fax: 410-502-2067, gagnett1@jhmi.edu.

DISCLOSURES

There are no disclosures.

Conclusions—pSer31 is a likely candidate seed for the nucleation process leading to cardiac PAOs deposition. Desmin post-translational processing and misfolding constitute a new, attractive avenue for the diagnosis and treatment of the cardiac accumulation of toxic PAOs that can now be measured by PET in acquired HF.

Keywords

Desmin; heart failure; preamyloid oligomers; post-translational modifications; pressure overload; amyloid

Subject Terms

Basic Science Research; Heart Failure; Nuclear Cardiology and PET

INTRODUCTION

Formation of preamyloid oligomers (PAOs) is emerging as a common hallmark of experimental and human acquired heart failure (HF)^{1–5}. Regardless of their sequence and disease, the vast majority of known PAOs are generated by post-translational processing of organ- and disease-specific protein sequences (e.g. A β 1–42 in Alzheimer's, α -synuclein and tau in Parkinson's, etc.). Typically, post-translational modifications (PTMs) generate the seed that initiates the nucleation process that leads to the formation of toxic PAOs and later fibrils and aggregates⁶. Preamyloid oligomers better predict organ dysfunction than large aggregates in Alzheimer's disease^{7, 8}; however, in contrast to aggregates, PAOs cannot be detected in the absence of specific staining or conformational antibodies⁶.

We previously reported that desmin phosphorylation and cleavage associate with the formation of cardiac PAOs and aggregates *in vitro*⁹ and *in vivo*¹. The finding that desmin forms PAOs when its main chaperone (α -B-crystallin or cryAB)³ is non-functional, suggests a mechanism independent from genetic mutations in desmin's sequence. It rather supports the notion that PAOs formation is facilitated by signaling pathways impacting PTMs, and that it exacerbates the cellular toxicity induced by proteostasis insufficiency, which characterizes HF^{3, 10}. Here, we focus on the role of PTMs in regulating protein misfolding and cardiac PAOs formation because they modulate desmin's physical properties and assembly^{1, 9, 11, 12}, as well as the formation of numerous well-characterized PAOs (e.g. Alzheimer's A β 1–42 phosphorylation and cleavage)^{6, 13}.

In this study, we tested whether cardiac PAOs accumulate in acquired HF and if pSer31-mimetic desmin promotes the formation of PAOs in cardiac myocytes. Further, we devised new protocols to track the build-up of PAOs *in vitro* and *in vivo*. To this end, we optimized a new method to purify, measure, and characterize amyloid in-gel, tested the effectiveness of a small molecule in reducing these species *in vitro*, and measured the build-up of cardiac PAOs in acquired HF *in vivo* by the unprecedented use of Positron Emission Tomography (PET).

METHODS

The data and methods supporting the findings in the manuscript are available from the corresponding author on reasonable request.

Animal and cellular models and human myocardial tissue

Transverse aortic constriction (TAC) and echocardiography were performed as previously described and in accordance with institutional guidelines¹⁴. Human myocardial tissue samples were obtained as described previously, under protocols approved by Institutional Review Boards at the University of Pennsylvania (PA, USA) and Johns Hopkins University (MD, US)¹⁵. Neonatal rat ventricular myocytes (NRVMs) isolation and lentiviral vectors production and infection were performed as described previously by Sekar and colleagues¹⁶. Details are provided in the online supplement.

Protein biochemistry

Protein extraction, western blot analysis and mass spectrometry (MS) were performed as described previously¹ with minor modifications described in the online supplement.

Live cell imaging

Living cells expressing desmin-GFP phosho-null/mimetic mutants were imaged using a spinning disc inverted confocal microscope equipped with two high-speed cameras (Olympus/Andor Revolution). Videos of living cells were acquired at a 40X magnification. Software assisted image analysis was performed using the Image J package, Fiji.

Filter assay

A filter assay to trap amyloid aggregates was used as we described⁹, with some modifications described in the online supplement.

Positron emission tomography (PET) and single-photon emission computed tomography (SPECT)

Please refer to the online supplement.

Statistical analysis

Data were normalized to the average of controls to correct for inter-experimental variability when appropriate. In this case, data were expressed as percentage arbitrary units (AU%). Student's *t*-test was applied for the comparison of two experimental groups while one-way ANOVA followed by Tukey's *post hoc* was used for the comparison of three groups. Statistical analyses were conducted using Prism 6 for Mac OS X (vers 6.b). All data are displayed as mean values \pm SD.

RESULTS

Desmin and PAOs co-migrate in experimental acquired HF

We previously reported the accumulation of cardiac PAOs in canine dyssynchronous HF¹, suggesting that these species can accumulate in the presence of cardiac, mechanical stress. To test if cardiac accumulation of PAOs occurs with acquired forms of HF we used transverse aortic constriction (TAC), one of the best established experimental models of HF¹⁷. Four weeks after TAC mice developed eccentric cardiac hypertrophy and overt HF as documented by heart weight, lung congestion, and echocardiography (Online Table I). We then combined western blot analysis with infrared fluorescence imaging (LI-COR) to simultaneously measure PAOs levels and their juxtaposition with desmin (Figure 1). The A11 antibody used here detects PAOs generated by different amyloidogenic sequences, such as A β , α -synuclein, prions, and others¹⁸. Since the only other common feature among these species is toxicity, the antibody recognizes an epitope responsible for their toxicity (=toxic epitope)¹⁸. We first detected the concurrent increase in the formation of PAOs and desmin cleavage in TAC mice vs. controls (≈ 2.5 -fold, $P=0.0006$ and ≈ 2 -fold, $P=0.006$, respectively, Figure 1A–C). We also found that wild-type desmin co-enriches and co-migrates with PAOs in this model (Figure 1A), and confirmed desmin cleavage by MS (Online Figure I).

Desmin cardiac PAOs accumulate in human HF

To address the clinical relevance of these findings we tested whether PAOs accumulate in human bioptic samples from dilated (non-ischemic, DCM, Figure 1D–F) and ischemic (ICM) cardiomyopathy (Figure 1G–I). Using the same double-staining approach we confirmed a ≈ 2 -fold increase of both cardiac desmin PAOs ($P=0.0366$, Figure 1E) and desmin cleavage ($P=0.0270$, Figure 1F) in DCM patients compared to non-failing (NF) controls. Intriguingly, our approach was able to differentiate DCM from ICM patients. In fact, a ≈ 3 -fold increase in the A11 signal at ≈ 190 kDa (compatible with short fibrils, see below) but not 55 kDa, was observed in ICM patients compared to controls ($P=0.00164$, Figure 1H), along with a ≈ 4 -fold increase in desmin cleavage ($P=0.0691$, Figure 1I). These data suggest that, though amyloid accumulation may represent a common denominator in different types of acquired, human HF, it is possible that the mechanisms and dynamics of their formation may vary. Follow-up studies that include a larger sample size are warranted to generalize the validity of these findings.

Epigallocatechin gallate de-aggregates wild type desmin PAOs in proteotoxic HF

In order to allow direct, downstream mass spectrometry (MS), we developed a novel staining approach based on a widely-used histological stain for amyloid, Thioflavin T (ThT)¹, and optimized it for classical, reducing SDS-PAGE (Figure 2A–B). We first validated the robustness of the method using cardiac extracts from R120G α -B-crystallin (cryAB) mice, a well-established model of cardiac proteotoxicity. The native desmin sequence is conserved and Robbins' group demonstrated a causal relationship between PAOs and HF development in these animals¹⁹. Using our new in-gel stain, we detected a ≈ 5 -fold increase in the ThT-positive signal compatible with desmin ($P=0.0005$). The specificity of the staining was confirmed by a $\approx 50\%$ decrease in the fluorescent signal upon treatment of the cardiac extracts with 20 μ M epigallocatechin gallate (EGCG, Figure 2B, $P=0.0196$), which disrupts

amyloid species^{1, 20}. Lastly, we confirmed desmin's presence in the ThT-positive bands by MS (Online Figure II). Taken together, these findings suggest that in a model of proteostasis insufficiency, where desmin's main chaperone is mutated while its native sequence is conserved, WT desmin contributes to the generation of PAOs. It is likely that other players and mechanisms contribute to the generation of PAOs and we cannot exclude that desmin loss of function could play an important role in the process. These aspects will be addressed in follow-up studies. Regardless of the relative contribution of desmin gain vs. loss of function to the process, we believe that, the effectiveness of EGCG in reducing the levels of amyloid in vitro opens new avenues for the therapeutic assessment of this and other small molecules for HF patients.

We further confirmed the increase of desmin PAOs (≈ 9 -fold, $P=0.0003$, Figure 2C–D) in the same proteotoxic model (R120G cryAB mice) using the dual immunostaining approach described above. When compared to non-transgenic controls, these mice display amplified desmin cleavage and the resulting fragment disproportionally increases (≈ 28 -fold) with respect to intact desmin (Figure 2E–F). The A11 and the anti-cryAB antibodies are both raised in rabbit and therefore cannot be used jointly. We detected a faint A11 signal compatible with cryAB's molecular weight, which was up-regulated in R120G cryAB mice (data not shown). However, using the anti-desmin antibody as a reference, we show that cryAB does not seem to directly participate in the formation of desmin cardiac PAOs (Figure 2G–H).

Phosphorylation at Ser31 promotes desmin aggregation

We previously reported the accumulation of mono-phosphorylated cardiac desmin and characterized the first two phospho-sites (Ser-27 and -31) in canine and human HF¹. The two sites are part of a consensus sequence for glycogen synthase kinase 3 β (GSK3 β), a kinase that classically recognizes a phosphorylated substrate (e.g. pSer31) and phosphorylates a residue three amino acids upstream (e.g. Ser-27). We also reported that GSK3 β phosphorylates desmin in vitro¹ and know that GSK3 β is inhibited in canine dyssynchronous HF²¹. Therefore, we hypothesized that GSK3 β inhibition in HF leads to the accumulation of amyloidogenic pSer31 desmin. Consequently, if the bi-phosphorylated form is the physiological proteoform, it should be less prone to aggregation¹. To test these hypotheses, we created bi- and mono-phospho-mimetic desmin double mutants using site mutagenesis and overexpressed them in neonatal rat ventricular myocytes (NRVMs) using lentiviral vectors expressing CMV-driven and GFP-fused bi- and mono-phospho-mimetic desmin double mutants (S27D,S31D or DD; and S27A,S31D or AD). We found that in transduced cells, exogenous desmin accounts for $\approx 25\%$ of total desmin (Online Figure III), which well reflects the stoichiometry of phospho-desmin proteoforms in clinical samples¹. We then examined transduced cells by live imaging using confocal, spinning disk microscopy to measure the proportion of contracting cells and desmin incorporation at the Z-bands. Expression of the desmin double phospho-mimetic mutant (DD) resulted in the highest number of contracting cells after one week in culture ($P=0.032$ vs. WT and $P=0.0012$ vs. AD, Figure 3A). This behavior was mirrored by the highest degree of desmin incorporation at the Z-bands ($P=0.0001$ vs. WT and $P=0.0005$ vs. AD, Figure 3B–C). In keeping with our proposed model, this evidence suggests that the doubly phosphorylated

form is the physiological proteoform. Similarly, expression of pSer31 obligatory mono-phospho-mimetic desmin (AD) resulted in decreased Z-bands incorporation (Figure 3B), as well as an increased formation of desmin-positive aggregates by filter assay, indicating that this is a pathological proteoform ($P=0.012$, Figure 3D–E). Thioflavin T staining (newly combined here with the filter assay) independently confirmed the increased propensity of pSer31 desmin to aggregate (Figure 3E). Interestingly, the average frequency of spontaneous contraction in pSer31-mimetic cells was 21 to 48% elevated in these mutants compared to the other groups (DD, $P=0.0002$ and WT, $P<0.0001$, respectively, Online Figure IVA). We interpret this observation as a dysregulation of ion fluxes, in agreement with the known permeabilizing effect of re-constituted PAOs on isolated cardiac cells^{2, 22}. Lastly, we employed magnetic twist cytometry on isolated NRVMs to assess if desmin PTMs and aggregation result in a loss of function impacting cytoskeletal stability and cell biophysics. We found no significance difference in cell stiffness in pSer31-mimetic (AD) and double phospho-mimetic (DD) mutants compared to WT suggesting that loss of desmin function has no discernible contribution to the adverse phenotype observed in pSer31-mimetic mutants (Online Figure IVB).

Desmin amyloid is increased and detectable in pressure-overload HF in vivo

Positron Emission Tomography - Computed Tomography (PET-CT) is increasingly recognized as a viable alternative to invasive biopsies to diagnose genetic cardiac amyloidosis^{23, 24}, but to our knowledge it was never employed to measure cardiac amyloid deposition in non-genetic HF before. Therefore, we used PET imaging for the unprecedented assessment of the accumulation of cardiac PAOs in vivo, in acquired HF. Notably, most of the tracers being investigated for the non-invasive, early detection of PAOs accumulation in Alzheimer's and Parkinson's diseases²⁵ are chemical derivatives of ThT. This chemical homology allowed us to correlate our PET data with those from the ThT in-gel stain assay.

To test our hypothesis that PAOs are formed in acquired HF in vivo, we injected 4-week TAC and sham operated mice each with 200 μCi of [¹⁸F] Amyvid® and imaged them using PET-CT. We found a significant, $13\% \pm 4.2$ increase in [¹⁸F] Amyvid® cardiac up-take in TAC mice compared to sham controls ($P=0.0194$), confirming the ex vivo data on increased PAOs accumulation in HF (Figure 4A–B). There were no differences in regional perfusion as determined by the SPECT tracer Cardiolite, ruling out increased Amyvid® uptake due to differences in regional myocardial blood flow (Figure 4A). Due to the chemical similarity between Amyvid® and ThT, it is likely that the tracer identifies the same desmin PAOs and short fibrils that we detected with our ThT in-gel stain.

Indeed, when we analyzed cardiac extracts from TAC mice and controls a ThT-positive band was increased in TAC mice myocardia vs. controls (≈ 3 -fold, $P=0.0005$) and reduced upon treatment with EGCG ($\approx 21\%$, $P=0.246$, Figure 4C–D). We confirmed the presence of desmin in this band, which is compatible with short fibrils, by MS (Online Figure V).

This evidence, combined with the data on the amyloidogenic potential of pSer31-mimetic desmin, supports the notion that post-translationally modified desmin acts as the seed for the

nucleation of cardiac PAOs in acquired heart failure in vivo, as well as the potential diagnostic applications of our findings.

DISCUSSION

Our study demonstrates that cardiac desmin PAOs accumulate in murine, pressure overload-induced and in human HF. Combined with the marked accumulation of desmin PAOs in a model of chaperone insufficiency (R120G cryAB mice), these data suggest that desmin PTMs, much like protein mutations, facilitate misfolding of desmin in the failing heart. This hypothesis draws further support from the present data showing that pSer31 phosphomimetic desmin has an increased propensity to aggregate and that this is toxic for isolated cells. This study also allowed us to refine our newly developed in-gel stain for amyloid as well as first combining Thioflavin T with a filter assay to confirm the amyloid nature of protein aggregates separated with these methods. From the translational standpoint, we provide proof of concept on the efficacy of EGCG in de-aggregating amyloid in pressure overload-induced and proteotoxic HF. Furthermore, we successfully measured the accumulation of PAOs in a well-established experimental model of acquired HF (TAC), non-invasively, using PET-CT for the first time. Therefore, PET could constitute a viable, non-invasive tool to monitor PAOs formation, as well as their potential therapeutic reduction in acquired HF, in vivo.

Desmin is the major component of intermediate filaments (IFs) in cardiac myocytes²⁶. Unlike the other components of the cytoskeleton (microtubules and actin filaments), IFs are constituted by distinct proteins in different cell types, which arguably hampered the creation of a unified vision on their function. In muscle cells, IFs have classically been viewed as mere scaffolds, maintaining sarcomeric alignment and the relative positioning of different organelles^{27, 28}. However, recent studies report numerous new functions for IFs in different cells types, including cardiac myocytes^{26, 29, 30}. The general consensus is that IFs were selected by evolution to confer protection against acute, mechanical stress in multicellular organisms without an exoskeleton. We propose that in the heart, this advantage came at a cost that is revealed under extended chronic stress: the formation of toxic PAOs. We and others demonstrated the accumulation of PAOs in clinical and experimental HF^{1–5, 22}. However, the modality of formation of these species in the heart is unknown to date and unlike other established proteinopathies (Alzheimer's, Parkinson's. etc.), the seed that initiates the nucleation process leading to cardiac PAOs formation remains the object of debate in acquired forms of HF⁶. The only mechanistic studies to our knowledge include that of Del Monte and colleagues, who recently demonstrated the accumulation of cofilin-2- or presenilin-positive PAOs in subsets of idiopathic dilated cardiomyopathy patients^{2, 5}, and work from Despa and colleagues reporting amylin PAOs in models of diabetic cardiomyopathy²². Here, we demonstrate that experimental, non-genetic models such as pressure-overload and human ischemic and non-ischemic HF share the accumulation of desmin PAOs. In light of the evolutionary role played by IFs in the response to stress, it is tempting to speculate that the formation of desmin PAOs may represent a general mechanism of adaptation to cardiac overload.

Light-chain and transthyretin (TTR) amyloidosis (AL and ATTR, respectively) are two notorious examples of genetic cardiac amyloidosis where the mutation of a protein sequence or its overproduction trigger the massive accumulation of cardiac amyloid³¹. Although both are systemic amyloidosis, one of the organs that is most affected and usually determines prognosis is the heart³¹. Wild type TTR also generates amyloid in the aging heart, in what was formerly known as cardiac senile amyloidosis and is now referred to as wild type TTR amyloidosis (ATTRwt). The discovery that PTMs (e.g. oxidative) modulate the propensity of wild type TTR and its genetic variants to aggregate, provides a potential explanation of why amyloid accumulates later in life³² and corroborates our theory on the contribution of toxic PTMs, rather than genetic mutations, to cardiac protein misfolding^{1, 6, 9}.

The recent technological advances in the field of mass spectrometry have unveiled a mind-blowing heterogeneity of protein PTMs²⁷. There are currently about 500 different types of PTMs listed in protein databases resulting from either chemical (e.g. oxidation) or enzymatic (e.g. phosphorylation) reactions⁶. These two classes of PTMs modulate protein misfolding and are respectively sustained by physical factors such as exceedingly oxidative or reductive environments and/or chronic imbalance of signaling pathways, all of which are well documented in HF and other proteinopathies⁶. Therefore, we believe that the elucidation of the pathophysiological role of protein PTMs will greatly help our understanding of the molecular mechanisms underlying HF development.

Various evidence points to a protective role of EGCG in cardiovascular and neurodegenerative diseases^{33–35}. Our data on the ability of EGCG in de-aggregating cardiac amyloid in vitro, provide a new interpretation for the protective effects of polyphenols. Therefore, we believe that molecules that directly target cardiac PAOs formation could be of therapeutic value for HF patients. In fact, our new use of PET to measure cardiac PAOs non-invasively in acquired forms of HF demonstrates that PAOs are not artifacts due to protein extraction. From a translational standpoint, this exciting new application enables future studies addressing the temporal association between PAOs accumulation and cardiac dysfunction in vivo, as well as studies testing its diagnostic and prognostic applicability.

In conclusion, we report that desmin cleavage and phosphorylation contribute to the formation of cardiac aggregates and PAOs. Wild type desmin generates PAOs in murine and human HF. Combined with the increased propensity of pSer31 desmin to aggregate, this new evidence supports a model where mono-phosphorylated and potentially cleaved desmin is the seed priming the nucleation process that leads to the formation of cardiac PAOs in acquired HF. Further, this new knowledge opens a new avenue for the development of diagnostic and therapeutic tools for HF.

Supplementary Material

Refer to Web version on PubMed Central for supplementary material.

Acknowledgments

The Authors are grateful to their collaborators at JHU, particularly to Brian O'Rourke, and Soroosh Solhjoo; and to Kenneth Margulies and Kenneth Bedi at University of Pennsylvania for the human tissue.

SOURCES OF FUNDING

This study was funded by the NHLBI (R01 HL107361) to SAA, the American Heart Association (2SDG9210000 and 16IRG27240002), the Magic That Matters Foundation, the NHLBI (P01 HL107153) and RFO University of Bologna to GA.

Nonstandard Abbreviations and Acronyms

A	light-chain
CBB	coomassie brilliant blue
CMV	cytomegalovirus
cryAB	α -B-crystallin
CT	computed tomography
DB71	direct blue 71
EGCG	epigallocatechin gallate
GFP	green fluorescent protein
GSK3β	glycogen synthase kinase 3 β
Ifs	intermediate filaments
MS	mass spectrometry
NRVMs	neonatal rat ventricular myocytes
PAOs	pre-amyloid oligomers
PET	positron emission tomography
pSer31	Ser-31 phosphorylated
PTMs	post-translational modifications
SPECT	single-photon emission computed tomography
ThT	thioflavin T
TTR	transthyretin

References

1. Agnetti G, Halperin VL, Kirk JA, Chakir K, Guo Y, Lund L, Nicolini F, Gherli T, Guarnieri C, Caldarera CM, Tomaselli GF, Kass DA, Van Eyk JE. Desmin modifications associate with amyloid-like oligomers deposition in heart failure. *Cardiovasc Res*. 2014; 102:24–34. [PubMed: 24413773]
2. Gianni D, Li A, Tesco G, McKay KM, Moore J, Raygor K, Rota M, Gwathmey JK, Dec GW, Aretz T, Leri A, Semigran MJ, Anversa P, Macgillivray TE, Tanzi RE, del Monte F. Protein aggregates and novel presenilin gene variants in idiopathic dilated cardiomyopathy. *Circulation*. 2010; 121:1216–26. [PubMed: 20194882]

3. Sanbe A, Osinska H, Saffitz JE, Glabe CG, Kaye R, Maloyan A, Robbins J. Desmin-related cardiomyopathy in transgenic mice: a cardiac amyloidosis. *Proc Natl Acad Sci U S A*. 2004; 101:10132–6. [PubMed: 15220483]
4. Sidorova TN, Mace LC, Wells KS, Yermalitskaya LV, Su PF, Shyr Y, Byrne JG, Petracek MR, Greulich JP, Hoff SJ, Ball SK, Glabe CG, Brown NJ, Barnett JV, Murray KT. Quantitative Imaging of Preamyloid Oligomers, a Novel Structural Abnormality, in Human Atrial Samples. *J Histochem Cytochem*. 2014; 62:479–87. [PubMed: 24789805]
5. Subramanian K, Gianni D, Balla C, Assenza GE, Joshi M, Semigran MJ, Macgillivray TE, Van Eyk JE, Agnetti G, Paolucci N, Bamburg JR, Agrawal PB, Del Monte F. Cofilin-2 phosphorylation and sequestration in myocardial aggregates: novel pathogenetic mechanisms for idiopathic dilated cardiomyopathy. *J Am Coll Cardiol*. 2015; 65:1199–1214. [PubMed: 25814227]
6. Del Monte F, Agnetti G. Protein post-translational modifications and misfolding: new concepts in heart failure. *Proteomics Clin Appl*. 2014; 8:534–42. [PubMed: 24946239]
7. Demuro A, Smith M, Parker I. Single-channel Ca(2+) imaging implicates Abeta1–42 amyloid pores in Alzheimer's disease pathology. *J Cell Biol*. 2011; 195:515–24. [PubMed: 22024165]
8. Aleardi AM, Benard G, Augereau O, Malgat M, Talbot JC, Mazat JP, Letellier T, Dachary-Prigent J, Solaini GC, Rossignol R. Gradual alteration of mitochondrial structure and function by beta-amyloids: importance of membrane viscosity changes, energy deprivation, reactive oxygen species production, and cytochrome c release. *J Bioenerg Biomembr*. 2005; 37:207–25. [PubMed: 16167177]
9. Agnetti G, Bezstarosti K, Dekkers DH, Verhoeven AJ, Giordano E, Guarnieri C, Caldarera CM, Van Eyk JE, Lamers JM. Proteomic profiling of endothelin-1-stimulated hypertrophic cardiomyocytes reveals the increase of four different desmin species and alpha-B-crystallin. *Biochim Biophys Acta*. 2008; 1784:1068–76. [PubMed: 18472024]
10. Willis MS, Patterson C. Proteotoxicity and cardiac dysfunction--Alzheimer's disease of the heart? *N Engl J Med*. 2013; 368:455–64. [PubMed: 23363499]
11. Geisler N, Weber K. Phosphorylation of desmin in vitro inhibits formation of intermediate filaments; identification of three kinase A sites in the aminoterminal head domain. *EMBO J*. 1988; 7:15–20. [PubMed: 3359992]
12. Nelson WJ, Traub P. Proteolysis of vimentin and desmin by the Ca2+-activated proteinase specific for these intermediate filament proteins. *Mol Cell Biol*. 1983; 3:1146–56. [PubMed: 6308428]
13. Kumar S, Rezaei-Ghaleh N, Terwel D, Thal DR, Richard M, Hoch M, McDonald JM, Wullner U, Glebov K, Heneka MT, Walsh DM, Zweckstetter M, Walter J. Extracellular phosphorylation of the amyloid beta-peptide promotes formation of toxic aggregates during the pathogenesis of Alzheimer's disease. *EMBO J*. 2011; 30:2255–65. [PubMed: 21527912]
14. Kaludercic N, Carpi A, Nagayama T, Sivakumaran V, Zhu G, Lai EW, Bedja D, De Mario A, Chen K, Gabrielson KL, Lindsey ML, Pacak K, Takimoto E, Shih JC, Kass DA, Di Lisa F, Paolucci N. Monoamine oxidase B prompts mitochondrial and cardiac dysfunction in pressure overloaded hearts. *Antioxid Redox Signal*. 2014; 20:267–80. [PubMed: 23581564]
15. Lee DI, Zhu G, Sasaki T, Cho GS, Hamdani N, Holewinski R, Jo SH, Danner T, Zhang M, Rainer PP, Bedja D, Kirk JA, Ranek MJ, Dostmann WR, Kwon C, Margulies KB, Van Eyk JE, Paulus WJ, Takimoto E, Kass DA. Phosphodiesterase 9A controls nitric-oxide-independent cGMP and hypertrophic heart disease. *Nature*. 2015; 519:472–6. [PubMed: 25799991]
16. Sekar RB, Kizana E, Smith RR, Barth AS, Zhang Y, Marban E, Tung L. Lentiviral vector-mediated expression of GFP or Kir2.1 alters the electrophysiology of neonatal rat ventricular myocytes without inducing cytotoxicity. *Am J Physiol Heart Circ Physiol*. 2007; 293:H2757–70. [PubMed: 17675572]
17. Houser SR, Margulies KB, Murphy AM, Spinale FG, Francis GS, Prabhu SD, Rockman HA, Kass DA, Molkentin JD, Sussman MA, Koch WJ. American Heart Association Council on Basic Cardiovascular Sciences CoCC, Council on Functional G, Translational B. Animal models of heart failure: a scientific statement from the American Heart Association. *Circ Res*. 2012; 111:131–50. [PubMed: 22595296]
18. Kaye R, Head E, Thompson JL, McIntire TM, Milton SC, Cotman CW, Glabe CG. Common structure of soluble amyloid oligomers implies common mechanism of pathogenesis. *Science*. 2003; 300:486–9. [PubMed: 12702875]

19. Pattison JS, Sanbe A, Maloyan A, Osinska H, Klevitsky R, Robbins J. Cardiomyocyte expression of a polyglutamine preamyloid oligomer causes heart failure. *Circulation*. 2008; 117:2743–51. [PubMed: 18490523]
20. Roberts BE, Duennwald ML, Wang H, Chung C, Lopreiato NP, Sweeny EA, Knight MN, Shorter J. A synergistic small-molecule combination directly eradicates diverse prion strain structures. *Nat Chem Biol*. 2009; 5:936–46. [PubMed: 19915541]
21. Chakir K, Daya SK, Tunin RS, Helm RH, Byrne MJ, Dimaano VL, Lardo AC, Abraham TP, Tomaselli GF, Kass DA. Reversal of global apoptosis and regional stress kinase activation by cardiac resynchronization. *Circulation*. 2008; 117:1369–77. [PubMed: 18316490]
22. Despa S, Margulies KB, Chen L, Knowlton AA, Havel PJ, Taegtmeier H, Bers DM, Despa F. Hyperamylinemia contributes to cardiac dysfunction in obesity and diabetes: a study in humans and rats. *Circ Res*. 2012; 110:598–608. [PubMed: 22275486]
23. Antoni G, Lubberink M, Estrada S, Axelsson J, Carlson K, Lindsjo L, Kero T, Langstrom B, Granstam SO, Rosengren S, Vedin O, Wassberg C, Wikstrom G, Westermark P, Sorensen J. In vivo visualization of amyloid deposits in the heart with 11C-PIB and PET. *J Nucl Med*. 2013; 54:213–20. [PubMed: 23238792]
24. Pilebro B, Arvidsson S, Lindqvist P, Sundstrom T, Westermark P, Antoni G, Suhr O, Sorensen J. Positron emission tomography (PET) utilizing Pittsburgh compound B (PIB) for detection of amyloid heart deposits in hereditary transthyretin amyloidosis (ATTR). *J Nucl Cardiol*. 2018; 25:240–248. [PubMed: 27645889]
25. Romano M, Buratti E. Florbetapir F 18 for brain imaging of beta-amyloid plaques. *Drugs Today (Barc)*. 2013; 49:181–93. [PubMed: 23527322]
26. Diokmetzidou A, Soumaka E, Kloukina I, Tsikitis M, Makridakis M, Varela A, Davos CH, Georgopoulos S, Anesti V, Vlahou A, Capetanaki Y. Desmin and alphaB-crystallin interplay in the maintenance of mitochondrial homeostasis and cardiomyocyte survival. *J Cell Sci*. 2016; 129:3705–3720. [PubMed: 27566162]
27. Agnetti G, Husberg C, Van Eyk JE. Divide and conquer: the application of organelle proteomics to heart failure. *Circ Res*. 2011; 108:512–26. [PubMed: 21335433]
28. Schwarz N, Leube RE. Intermediate Filaments as Organizers of Cellular Space: How They Affect Mitochondrial Structure and Function. *Cells*. 2016:5.
29. Coulombe PA, Wong P. Cytoplasmic intermediate filaments revealed as dynamic and multipurpose scaffolds. *Nat Cell Biol*. 2004; 6:699–706. [PubMed: 15303099]
30. Hnia K, Ramspacher C, Vermot J, Laporte J. Desmin in muscle and associated diseases: beyond the structural function. *Cell Tissue Res*. 2015; 360:591–608. [PubMed: 25358400]
31. Ablasser K, Verheyen N, Glantschnig T, Agnetti G, Rainer PP. Unfolding Cardiac Amyloidosis - From Pathophysiology to Cure. *Curr Med Chem*. 2018
32. Zhao L, Buxbaum JN, Reixach N. Age-related oxidative modifications of transthyretin modulate its amyloidogenicity. *Biochemistry*. 2013; 52:1913–26. [PubMed: 23414091]
33. Lee JW, Lee YK, Ban JO, Ha TY, Yun YP, Han SB, Oh KW, Hong JT. Green tea (-)-epigallocatechin-3-gallate inhibits beta-amyloid-induced cognitive dysfunction through modification of secretase activity via inhibition of ERK and NF-kappaB pathways in mice. *J Nutr*. 2009; 139:1987–93. [PubMed: 19656855]
34. Oyama JI, Shiraki A, Nishikido T, Maeda T, Komoda H, Shimizu T, Makino N, Node K. EGCG, a green tea catechin, attenuates the progression of heart failure induced by the heart/muscle-specific deletion of MnSOD in mice. *J Cardiol*. 2017; 69:417–427. [PubMed: 27374189]
35. Wolfram S. Effects of green tea and EGCG on cardiovascular and metabolic health. *J Am Coll Nutr*. 2007; 26:373S–388S. [PubMed: 17906191]

Novelty and Significance

What Is Known?

- Pre-amyloid oligomers (PAOs), similar to those observed in the brain of patients with Alzheimer's and Parkinson's diseases, accumulate in human heart failure.
- PAOs are toxic to isolated cardiac myocytes and they cause heart failure in transgenic mouse models.
- The mechanisms of cardiac PAOs formation in acquired (non-genetic) forms of heart failure are unclear.

What New Information Does This Article Contribute?

- Using a dual immunostaining approach and a novel in-gel staining for amyloid coupled with mass spectrometry, we show that cardiac PAOs and short-fibrils containing the cytoskeletal protein desmin accumulate in murine and human acquired heart failure.
- The small molecule epigallocatechin gallate (EGCG) is able to de-aggregate cardiac PAOs and short fibrils in vitro.
- Positron emission tomography is able to detect the increased levels of cardiac amyloid in murine acquired heart failure in vivo, in a non-invasive fashion.

Heart failure represents the common end stage of a number of cardiac morbidities and is on the rise. The mechanisms underlying the transition from compensated left ventricle (LV) hypertrophy to maladaptive cardiac remodeling and failure remain ill defined. The observation that many forms of heart failure share impaired proteostasis, regardless of their etiology, highlights the pivotal role of protein misfolding in this transition. Although protein mutations trigger the deposition of cardiac amyloid, our data suggest that a modified form of the cytoskeletal protein desmin acts as a nucleating seed in the formation of toxic PAOs in the heart, in the absence of any genetic mutation. We used new methodologies, and optimized existing ones to specifically and accurately detect PAOs ex vivo and in vivo. Importantly, we report that epigallocatechin gallate cande-aggregates cardiac amyloid in vitro.

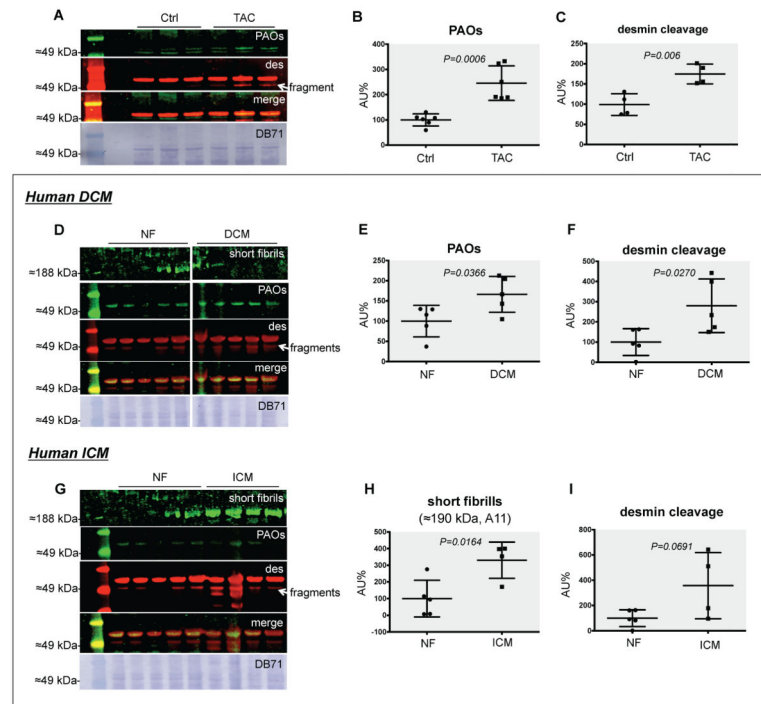


Figure 1. Desmin PAOs accumulate in experimental and human HF

PAOs (green, A11) and desmin (des, red) detected by western blot analysis: PAOs co-migrated with desmin in myofilament-enriched protein homogenates from TAC mouse hearts (A). Densitometry highlighted a ≈ 2.5 -fold increase in PAOs ($P=0.0006$, $N=6$ each, B) and a ≈ 2 -fold increase in desmin cleavage ($P=0.006$, $N=4$ each, C) in TAC vs. sham control (Ctrl) mice. A ≈ 2 -fold increase of both desmin PAOs ($P=0.0366$, $N=5$ each, D–E) and desmin cleavage ($P=0.0270$, $N=5$ each, F) was also observed in dilated (non-ischemic) cardiomyopathy (DCM) compared to non-failing (NF) human hearts. A ≈ 3 -fold increase in the A11 signal at ≈ 190 kDa, compatible with short fibrils, was evident in ischemic cardiomyopathy (ICM) patients compared to NF controls ($P=0.00164$, $N=5/4$ each G–H), along with a ≈ 4 -fold increase in desmin cleavage ($P=0.0691$, $N=5/4$ each, I). An image of the total protein stain by direct blue 71 (DB71, Sigma) is also provided for every blot.

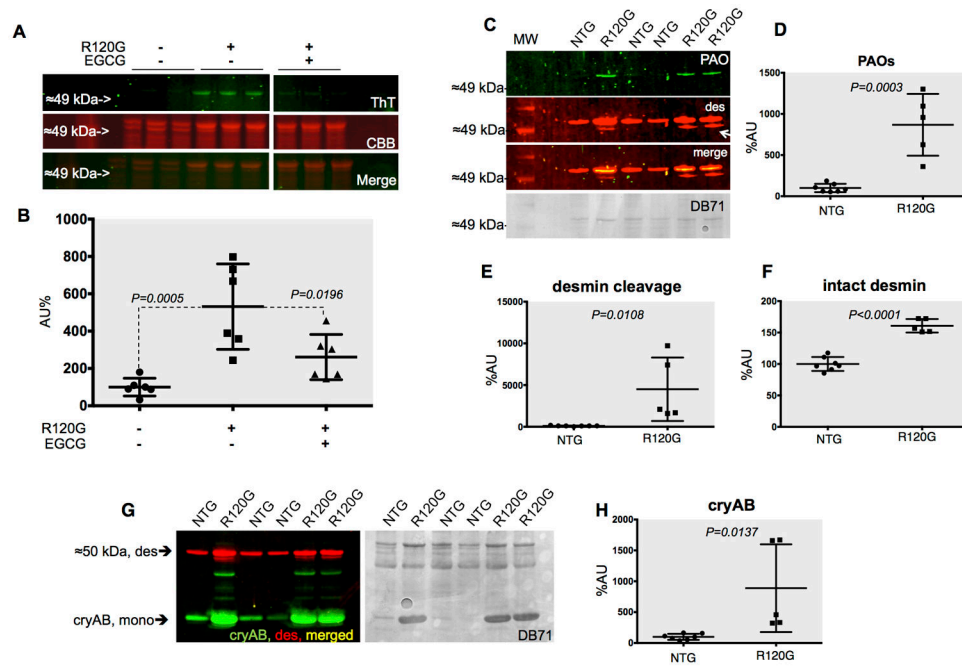


Figure 2. Wild type desmin generates PAOs in cryAB mice

We used Thioflavin T (ThT) in-gel stain to analyze cardiac extracts from R120G cryAB mice (R120G) and non-transgenic (NTG) controls under denaturing conditions. Protein extracts were incubated with EGCG or vehicle (DMSO) to improve specificity (**A**). Densitometry revealed a ~ 5 -fold increase in a ThT-positive band at ~ 55 kDa in R120G cryAB samples compared to non-transgenic controls ($P=0.0005$, $N=6$ each). EGCG treatment resulted in a $\sim 50\%$ reduction in amyloid, ThT-positive signal ($P=0.0196$, $N=6$ each, **B**). CBB, Coomassie brilliant blue. The same samples were analyzed by western blot using dual staining for PAOs (green) and desmin (des, red, **C**). Densitometry revealed a ~ 9 -fold increase in desmin PAOs ($P=0.0003$, $N=7/5$ each, **C–D**) as well as a relative increase of ~ 28 -fold in desmin cleavage compared to intact desmin ($N=7/5$ each, **E–F**). Lastly, a ~ 9 -fold increase in cryAB was observed in R120G vs. NTG ($P=0.0137$, $N=7/5$ each, **G–H**) although this signal did not overlap with that of desmin (or hence its PAOs). An image of the total protein stain by direct blue 71 (DB71, Sigma) is also provided for every blot.

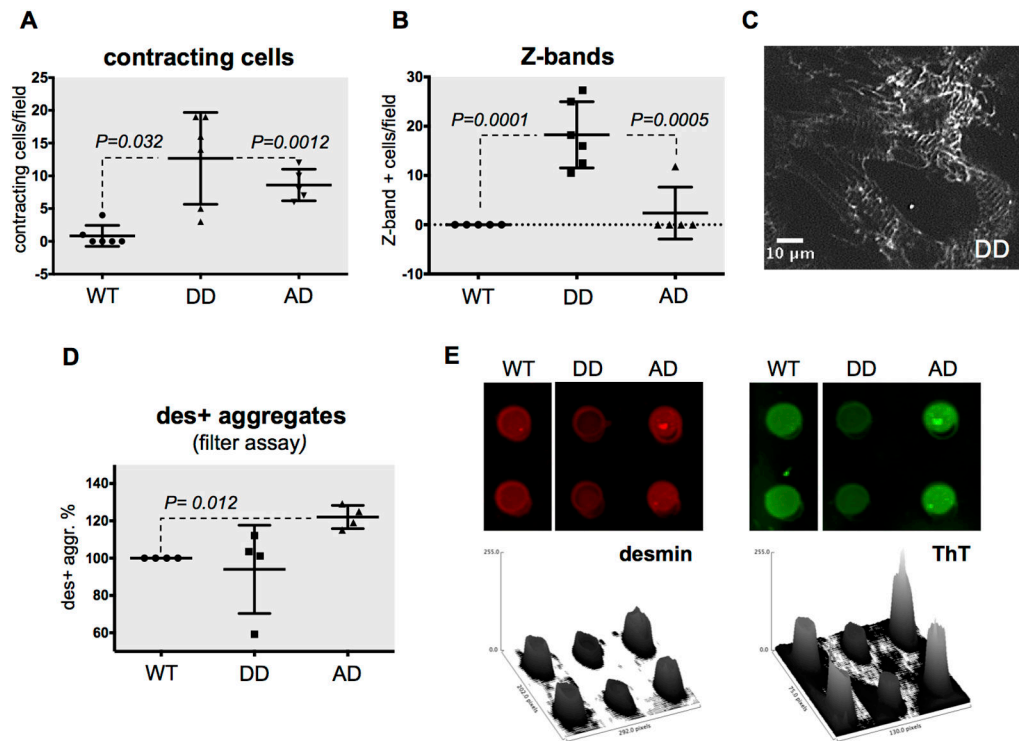


Figure 3. Functional analysis of NRVMs transduced with phospho-mimetic desmin

Neonatal rat ventricular myocytes transduced with fluorescently-tagged desmin phospho-mimetic/null mutants for Ser-27 and -31 (S27D, S31D or DD; and S27A, S31D or AD) as well as wild-type desmin were live imaged. Every data point represents a confocal field, hence tens of cells. Videos were automatically analyzed to measure: contracting cells (**A**) and desmin Z-bands incorporation (**B**). A representative picture of DD mutants showing striation is provided in (**C**). Desmin positive aggregates were also measured by filter assay (N=4 each, **D–E**), and the amyloid nature of these aggregates was confirmed using Thioflavin T (ThT, **E**).

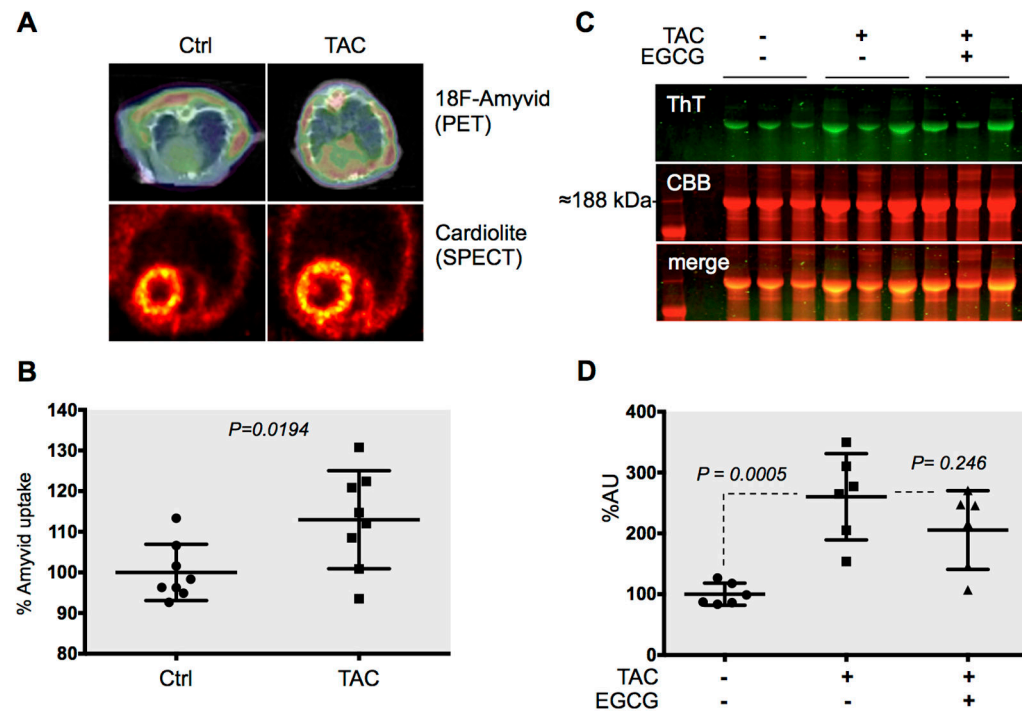


Figure 4. Amyloid accumulation in pressure overload HF as detected non-invasively by Positron Emission Tomography (PET) and ex vivo by ThT in-gel stain

Four-week TAC mice and sham controls were injected with the amyloid PET-tracer Amyvid and imaged by PET. Representative images of the tracer signal, superimposed on CT scans are provided (**A top**). The SPECT tracer Cardiolite was used to rule out difference in myocardial blood flow. Normalized Amyvid uptake was analyzed (N=8 each, **A bottom**). Thioflavin T (ThT) in-gel stain confirmed a ≈ 3 -fold increase in short, fibrillar amyloid *ex-vivo* ($P=0.0005$, N=6 each, **C**). The presence of desmin in these bands was confirmed by MS (Online Figure V). A $\approx 21\%$ decrease in the ThT signal upon treatment with epigallocatechin gallate (EGCG) confirmed the specificity of the stain (**C–D**).